A layered compensation optimization strategy of energy storage type railway power conditioner

YING WANG[1], YANQIANG HE[1] ⊠, XIAOQIANG CHEN[1], MIAOMIAO ZHAO[1], JING XIE[2]

[1]*School of Automation and Electrical Engineering*
Lanzhou Jiaotong University
Lanzhou,730070 China

[2]*Xi'an Rail Transit Group Co., LTD*
Operation Branch
Xi'an, 710000 China

e-mail: *wangying01@lzjtu.edu.cn,* ⊠*yanqiang_he@foxmail.com*

Abstract: Aiming at the problems of the negative sequence governance and regenerative braking energy utilization of electrified railways, a layered compensation optimization strategy considering the power flow of energy storage systems was proposed based on the railway power conditioner. The paper introduces the topology of the energy storage type railway power conditioner, and analyzes its negative sequence compensation and regenerative braking energy utilization mechanism. Considering the influence of equipment capacity and power flow of the energy storage system on railway power conditioner compensation effect, the objective function and constraint conditions of the layered compensation optimization of the energy storage type railway power conditioner were constructed, and the sequential quadratic programming method was used to solve the problem. The feasibility of the proposed strategy is verified by a multi-condition simulation test. The results show that the proposed optimization compensation strategy can realize negative sequence compensation and regenerative braking energy utilization, improve the power factor of traction substations when the system equipment capacity is limited, and it also has good real-time performance.

Key words: electrified railway, energy storage system negative sequential governance, railway power conditioner, regenerative braking energy

1. Introduction

With the development of high speed and heavy loads of electrified railways, negative sequence and regenerative braking energy have gradually become the important factors that restrict the green and energy-saving development of electrified railways and the safe and stable operation [1, 2].

In terms of reducing the negative sequence current of electrified railways, the railway power conditioner (RPC) has been paid much attention by many scholars because it is capable of transferring the active power of two supply arms and compensating the reactive power to fully compensate the negative sequence current component of three-phase traction substations [3, 4]. In [5], the system stability of the RPC with an LCL filter is analyzed, and the corresponding converter control strategy is proposed. An optimization strategy of the RPC negative sequence current compensation under multiple constraints is proposed in [6], and the real-time performance of the solution algorithm is analyzed. [7] takes the Italian railway as an example to discuss the economic problem of using the energy storage system to recover regenerative braking energy along the railway. Based on the idea of using the energy storage system to suppress power fluctuation [8, 9], some scholars proposed to add the energy storage system (ESS) in the DC side of the RPC to realize the negative sequence current compensation and utilization of braking regenerative energy [10–12]. However, the addition of the ESS will introduce a new energy flow on the DC side of the RPC, the negative sequence current complete compensation strategy for the energy storage type RPC (ESRPC) system is reformulated in [13]. The RPC control strategy based on the ultracapacitor energy storage system is proposed in [14], and a multi-source energy management strategy for the energy storage system and new energy access to the traction power supply system is proposed in [15]. To sum up, the current researches on the ESRPC are mostly focused on the topology of the ESRPC, negative sequence complete compensation method and corresponding converter control strategy, and there are few researches on compensation optimization considering the limited capacity of ESRPC equipment.

In this paper, the structure of the ESRPC system is introduced, and the mechanism of ESRPC negative sequence compensation and regenerative braking energy utilization is analyzed. The layered compensation optimization method of the ESRPC was proposed, and the charging and discharging strategy of the ESS and the compensation optimization mathematical model of the ESRPC under limited equipment capacity were established. The model was solved by using the sequential quadratic programming (SQP) method. Finally, through the simulation model, the proposed strategy is tested from multiple perspectives, and the feasibility and effectiveness of the proposed strategy are verified.

2. Energy storage railway power conditioner system topology

The system topology of the ESRPC is shown in Fig. 1. The 110 kV three-phase alternating voltage of the AC power grid is stepped down into two single-phase power supply sources at a rank of 27.5 kV by a V/v transformer, and the two power supply arms of α and β are respectively used to provide electric energy for train driving. The RPC is composed of two back-to-back converters VSC_{α}, VSC_{β} and the intermediate DC side supporting capacitor C. The two converters are respectively connected to the outlets of α and β power supply arms through the step-down transformers T_{α} and T_{β}. The ESS is made of an energy storage medium and a bidirectional

DC/DC converter. The energy storage medium is connected to the DC side of the RPC through a bidirectional DC/DC converter. Among them, the RPC system communicates with the two power supply arms of α and β, balances the active power of the two arms, and adjusts the reactive power. At the same time, it is also the hub of power exchange between the energy storage system and the two power supply arms of α and β. The energy storage system must go through the two RPC converters VSC$_\alpha$ and VSC$_\beta$ to realize the recovery and utilization of the regenerative braking energy of the two power supply arms and reduce the peak power demand during the traction of the two arms. To simplify the analysis process, system losses and efficiency differences between components are ignored.
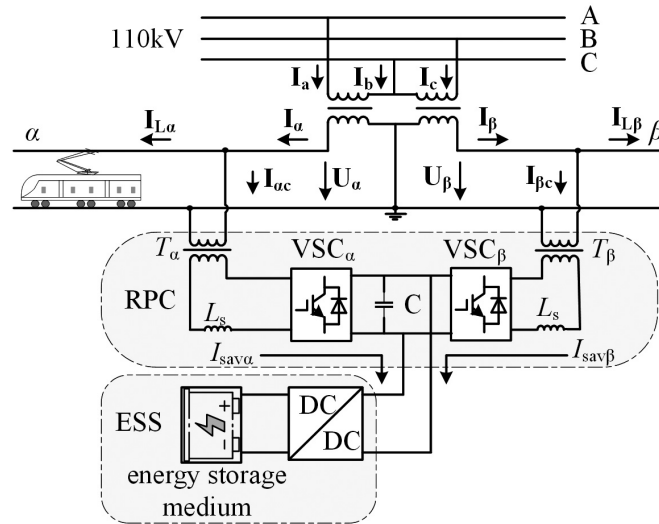

Fig. 1. ESRPC system structure

3. The negative sequence compensation and regenerative braking energy utilization mechanism of ESRPC

Let's assume that in the system structure shown in Fig. 1, the voltages of the two power supply arms α and β are:

$$\begin{cases} \boldsymbol{U_\alpha} = U_\alpha\, e^{i-\left(\frac{\pi}{6}\right)} \\ \boldsymbol{U_\beta} = U_\beta\, e^{i-\left(\frac{\pi}{2}\right)} \end{cases}, \tag{1}$$

where U_α and U_β are the rms voltages of the two power supply arms and $U_\alpha = U_\beta$.

Without considering harmonics, the load currents of the two power supply arms are:

$$\begin{cases} \boldsymbol{I_{L\alpha}} = I_{L\alpha}\, e^{i\left(-\frac{\pi}{6}-\theta_{L\alpha}\right)} \\ \boldsymbol{I_{L\beta}} = I_{L\beta}\, e^{i\left(-\frac{\pi}{2}-\theta_{L\beta}\right)} \end{cases}, \tag{2}$$

where: $I_{L\alpha}$ and $I_{L\beta}$ are the rms values of the load currents of the two power supply arms, respectively; $\theta_{L\alpha}$ and $\theta_{L\beta}$ are the power factor angles of the two arms respectively.

In Figure 1, assuming that after conversion to the primary sides of T_α and T_β, the active compensation currents provided by the energy storage system for the two power supply arms are $I_{\mathrm{sav}\alpha}$ and $I_{\mathrm{sav}\beta}$, then after compensation by the energy storage system, the load currents of the two power supply arms are:

$$\begin{cases} \boldsymbol{I'_{\mathbf{L}\alpha}} = \sqrt{\left(I_{\mathrm{L}\alpha\mathrm{d}} + I_{\mathrm{sav}\alpha}\right)^2 + I_{\mathrm{L}\alpha\mathrm{q}}^2}\, e^{j\left(-\frac{\pi}{6}-\theta_{\mathrm{L}\alpha}\right)} \\ \boldsymbol{I'_{\mathbf{L}\beta}} = \sqrt{\left(I_{\mathrm{L}\beta\mathrm{d}} + I_{\mathrm{sav}\beta}\right)^2 + I_{\mathrm{L}\beta\mathrm{q}}^2}\, e^{j\left(-\frac{\pi}{2}-\theta_{\mathrm{L}\beta}\right)} \end{cases}, \tag{3}$$

where: $I_{\mathrm{L}\alpha\mathrm{d}}$ and $I_{\mathrm{L}\beta\mathrm{d}}$ are the active components of the load currents in the two arms, respectively; $I_{\mathrm{L}\alpha\mathrm{q}}$ and $I_{\mathrm{L}\beta\mathrm{q}}$ are the reactive components of the load currents in the two arms, respectively.

From (3) it follows that if the active components of the load currents in the two arms of α and β are equal after compensation, then on the primary sides of T_α and T_β, the active compensation components $I_{\alpha\mathrm{cd}}$ and $I_{\beta\mathrm{cd}}$ provided by the ESRPC for the load current of the two power supply arms are:

$$\begin{cases} I_{\alpha\mathrm{cd}} = -0.5(I_{\mathrm{L}\alpha\mathrm{d}} - I_{\mathrm{L}\beta\mathrm{d}}) + 0.5(I_{\mathrm{sav}\alpha} + I_{\mathrm{sav}\beta}) \\ I_{\beta\mathrm{cd}} = 0.5(I_{\mathrm{L}\alpha\mathrm{d}} - I_{\mathrm{L}\beta\mathrm{d}}) + 0.5(I_{\mathrm{sav}\alpha} + I_{\mathrm{sav}\beta}) \end{cases}. \tag{4}$$

It can be seen from (4) that no matter what the active current $I_{\mathrm{sav}\alpha}$ and $I_{\mathrm{sav}\beta}$ compensated by the ESS to the two power supply arms, when the power flow is distributed on the DC side of the RPC, the active current compensated by the ESS to the two power supply arms is always the same. Therefore, when formulating the charging and discharging strategy of the energy storage system, only the total compensation current $I_{\mathrm{sav\,z}}$ of the ESS to the traction substation can be considered. At this point, $I_{\mathrm{sav\,z}}$ satisfies:

$$I_{\mathrm{sav\,z}} = I_{\mathrm{sav}\alpha} + I_{\mathrm{sav}\beta}\,. \tag{5}$$

Suppose that after ESRPC compensation, the load currents of the two power supply arms are:

$$\begin{cases} \boldsymbol{I_\alpha} = I_\alpha\, e^{i\left(-\frac{\pi}{6}-\theta_\alpha\right)} \\ \boldsymbol{I_\beta} = I_\beta\, e^{i\left(-\frac{\pi}{2}-\theta_\beta\right)} \end{cases}, \tag{6}$$

where: I_α and I_β are the rms values of the load currents of the two power supply arms after compensation, respectively; θ_α and θ_β are the power factor angles of the two arms after compensation respectively.

According to the symmetrical component method, the magnitude of the negative sequence current $I_{\mathrm{a}2}$ on the three-phase side of the traction substation after ESRPC compensation is:

$$I_{\mathrm{a}2} = \frac{\sqrt{3}}{3k}\sqrt{\left(I_\alpha\cos\left(\frac{\pi}{3}+\theta_\alpha\right) - I_\beta\cos\theta_\beta\right)^2 + \left(I_\beta\sin\theta_\beta - I_\alpha\sin\left(\frac{\pi}{3}+\theta_\alpha\right)\right)^2}, \tag{7}$$

where k is the ratio of the primary and secondary sides of the V/v connection traction transformer.

The rms values of the load currents of the two power supply arms after compensation can be expressed as:

$$\begin{cases} I_\alpha = \sqrt{\left(I_{\mathrm{L}\alpha\mathrm{d}} + I_{\alpha\mathrm{td}} + 0.5I_{\mathrm{sav\,z}}\right)^2 + \left(I_{\mathrm{L}\alpha\mathrm{q}} + I_{\alpha\mathrm{cq}}\right)^2} \\ I_\beta = \sqrt{\left(I_{\mathrm{L}\beta\mathrm{d}} + I_{\beta\mathrm{td}} + 0.5I_{\mathrm{sav\,z}}\right)^2 + \left(I_{\mathrm{L}\beta\mathrm{q}} + I_{\beta\mathrm{cq}}\right)^2} \end{cases}, \tag{8}$$

where $I_{\alpha\text{td}}$ and $I_{\beta\text{td}}$ are the transfer currents of the RPC between the two power supply arms, and both satisfy $I_{\alpha\text{td}} = -I_{\beta\text{td}}$.

From (7) and (8), it can be seen that if the $I_{\alpha\text{td}}$, $I_{\beta\text{td}}$, $I_{\alpha\text{cq}}$, $I_{\beta\text{cq}}$ and $I_{\text{sav z}}$ that make $I_{\text{a2}} \to 0$ can be obtained, the compensation for the negative sequence current on the three-phase side of the traction substation and the utilization of regenerative braking energy can be realized.

4. The layered compensation optimization strategy

The layered compensation optimization strategy of the ESRPC is shown in Fig. 2. Firstly, according to the dq coordinate components $I_{\text{L}\alpha\text{p}}$, $I_{\text{L}\beta\text{p}}$, $I_{\text{L}\alpha\text{q}}$ and $I_{\text{L}\beta\text{q}}$ of the load current on the two power supply arms of α and β, formulate the charging and discharging strategy of the energy storage system, determine the active current $I_{\text{sav z}}$ compensated by the ESS for the traction power supply system, and through the calculation of the DC/DC command current, the bidirectional DC/DC command current I_{sav} that controls the charging and discharging of the energy storage system is obtained; Secondly, considering the constraints of the ESRPC equipment capacity and the three-phase side power factor of the traction substation after compensation, the ESRPC compensation current is optimized with the goal of $I_{\text{a2}} \to 0$. Thus, the active currents $I_{\alpha\text{td}}$ and $I_{\beta\text{td}}$ that the RPC can transfer and the reactive currents $I_{\alpha\text{cq}}$ and $I_{\beta\text{cq}}$ that can be compensated are determined. Finally, $I_{\alpha\text{td}}$, $I_{\beta\text{td}}$, $I_{\alpha\text{cq}}$, $I_{\beta\text{cq}}$ and $I_{\text{sav z}}$ are combined into ESRPC two-port target current vectors $\boldsymbol{I}_{\text{mc}\alpha}$ and $\boldsymbol{I}_{\text{mc}\beta}$ as the command currents of the two back-to-back converters VSCα and VSCβ in Fig. 1. It is worth noting that, since the harmonic compensation process of the ESRPC is basically consistent with that of the RPC, and the compensation of the load fundamental wave current and the load harmonic current can be carried out separately, this paper only considers the optimization of the ESRPC fundamental wave compensation current, without considering harmonic compensation.
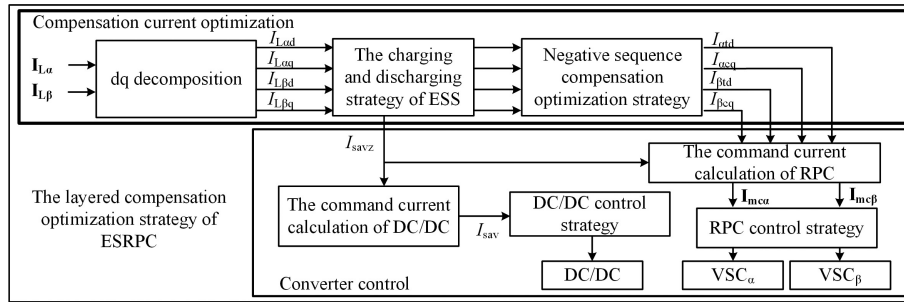

Fig. 2. The layered compensation optimization method of ESRPC

4.1. Energy storage system charging and discharging strategy

According to the load current active components $I_{\text{L}\alpha\text{d}}$ and $I_{\text{L}\beta\text{d}}$ of the two power supply arms and the state of charge (SOC) of the energy storage medium, the charging and discharging strategy shown in Fig. 3 is formulated to determine the compensation current $I_{\text{sav z}}$ of the energy storage system.
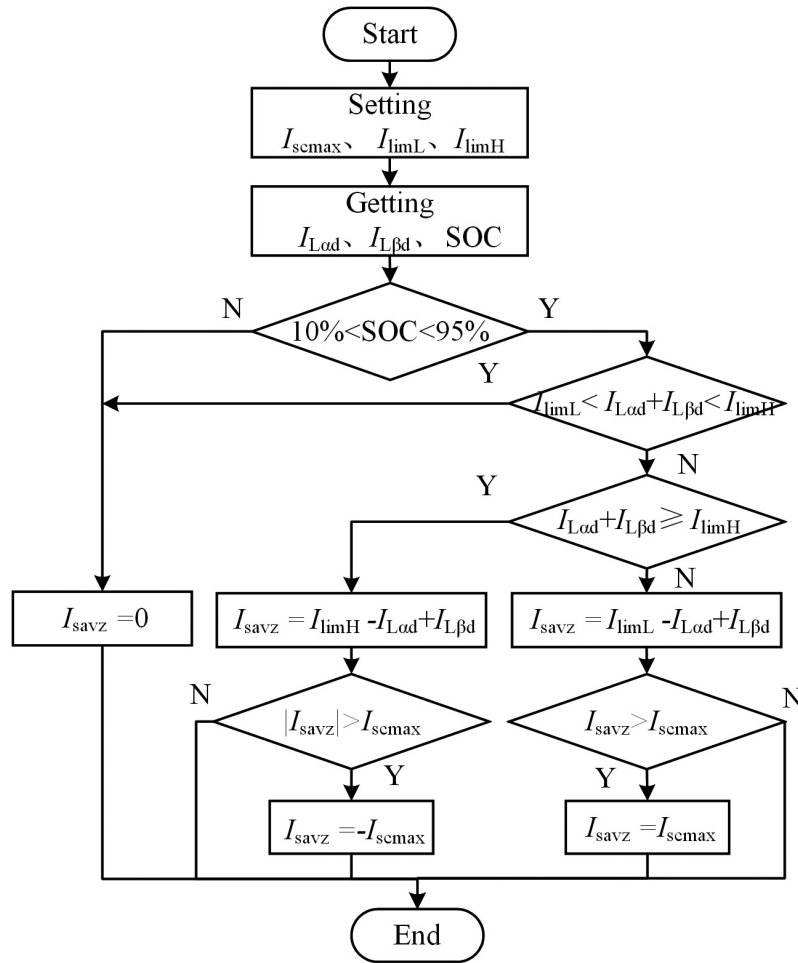
Fig. 3. Charging and discharging strategy of the energy storage system

In Figure 3, $I_{sc\,\max}$ is the maximum charge and discharge current of the energy storage system converted to the primary side of the step-down transformer T_α and T_β; $I_{\lim L}$ is the charge threshold of the energy storage system, and $I_{\lim H}$ is the discharge threshold of the energy storage system.

4.2. ESRPC compensation optimization strategy considering energy storage output

A. Objective function

Based on (4), define the active power compensation degree γ:

$$\gamma = -\frac{I_{t\alpha d}}{0.5\left(I_{L\alpha d} - I_{L\beta d}\right)} = \frac{I_{t\beta d}}{0.5\left(I_{L\alpha d} - I_{L\beta d}\right)}, \qquad \gamma \in [0,\ 1]. \tag{9}$$

In order to achieve the purpose of the ESRPC negative sequence compensation and regenerative braking energy utilization, the ESRPC optimization goal is determined as the problem of minimum negative sequence current when considering ESS output. Incorporating (8) and (9) into (7), the optimization objective function with γ, $I_{\alpha cq}$ and $I_{\beta cq}$ as decision variables can be determined as:

$$
\min I_{a2} = \frac{\sqrt{3}}{3k} \left(\begin{array}{l} \left(\begin{array}{l} \sqrt{\left(I_{L\alpha d} - 0.5\gamma\left(I_{L\alpha d} - I_{L\beta d}\right) + 0.5I_{\text{sav z}}\right)^2 + \left(I_{L\alpha q} + I_{\alpha cq}\right)^2} \\ \cos\left(\frac{\pi}{3} + \arctan\left(\frac{I_{L\alpha d} - I_{L\beta d}}{I_{L\alpha d} - 0.5\gamma\left(I_{L\alpha d} - I_{L\beta d}\right) + 0.5I_{\text{sav z}}}\right)\right) \\ -\sqrt{\left(I_{L\alpha d} - 0.5\gamma\left(I_{L\alpha d} - I_{L\beta d}\right) + 0.5I_{\text{sav z}}\right)^2 + \left(I_{L\alpha q} + I_{\alpha cq}\right)^2} \\ \cos\left(\frac{\pi}{3} + \arctan\left(\frac{I_{L\alpha d} - I_{L\beta d}}{I_{L\alpha d} - 0.5\gamma\left(I_{L\alpha d} - I_{L\beta d}\right) + 0.5I_{\text{sav z}}}\right)\right) \end{array} \right)^2 \\ + \left(\begin{array}{l} \sqrt{\left(I_{L\alpha d} - 0.5\gamma\left(I_{L\alpha d} - I_{L\beta d}\right) + 0.5I_{\text{sav z}}\right)^2 + \left(I_{L\alpha q} + I_{\alpha cq}\right)^2} \\ \sin\left(\frac{\pi}{3} + \arctan\left(\frac{I_{L\alpha d} - I_{L\beta d}}{I_{L\alpha d} - 0.5\gamma\left(I_{L\alpha d} - I_{L\beta d}\right) + 0.5I_{\text{sav z}}}\right)\right) \\ -\sqrt{\left(I_{L\alpha d} - 0.5\gamma\left(I_{L\alpha d} - I_{L\beta d}\right) + 0.5I_{\text{sav z}}\right)^2 + \left(I_{L\alpha q} + I_{\alpha cq}\right)^2} \\ \sin\left(\frac{\pi}{3} + \arctan\left(\frac{I_{L\alpha d} - I_{L\beta d}}{I_{L\alpha d} - 0.5\gamma\left(I_{L\alpha d} - I_{L\beta d}\right) + 0.5I_{\text{sav z}}}\right)\right) \end{array} \right)^2 \end{array} \right)^{1/2}. \quad (10)
$$

B. Constraint conditions

Suppose the equipment capacity of the RPC is S_{RPC}, then the equipment capacity constraints of the ESRPC system are:

$$
\begin{cases} \sqrt{\left[-0.5\gamma\left(I_{L\alpha d} - I_{L\beta d}\right) + 0.5I_{\text{sav z}}\right]^2 + I_{\alpha cq}^2} \le \dfrac{S_{\text{RPC}}}{U_\alpha} \\ \sqrt{\left[0.5\gamma\left(I_{L\alpha d} - I_{L\beta d}\right) + 0.5I_{\text{sav z}}\right]^2 + I_{\beta cq}^2} \le \dfrac{S_{\text{RPC}}}{U_\beta} \end{cases}. \quad (11)
$$

In order to avoid punitive charges due to too low power factor, the network-side power factor constraint conditions after ESRPC compensation should meet the following requirement:

$$
\frac{(P_\alpha + P_\beta)}{\sqrt{(P_\alpha + P_\beta)^2 + (Q_\alpha + Q_\beta)^2}} \ge Q_{\text{PF}}. \quad (12)
$$

According to (8) and (9), (12) can be rewritten as:

$$
\frac{1}{\sqrt{1 + \dfrac{\left(I_{L\alpha q} + I_{L\beta q} + I_{\alpha cq} + I_{\beta cq}\right)^2}{\left[I_{L\alpha d} - 0.5\gamma\left(I_{L\alpha d} - I_{L\beta d}\right) + 0.5I_{\text{sav z}}\right]^2 + \left[I_{L\beta d} + 0.5\gamma\left(I_{L\alpha d} - I_{L\beta d}\right) + 0.5I_{\text{sav z}}\right]^2}}} \ge Q_{\text{PF}}. \quad (13)
$$

It can be seen from (10) that the ESRPC compensation optimization model is a single-objective nonlinear programming model with multiple constraints. In order to meet the requirements of convergence accuracy and real-time performance, the sequential quadratic programming method [16] is used to solve the established optimization model to obtain γ, $I_{\alpha cq}$ and $I_{\beta cq}$ that satisfy the objective function and various constraints.

C. Calculation of converter command current

According to the charging and discharging strategy of the energy storage system and the compensation optimization model, the compensation currents $I_{\text{sav z}}$, $I_{\alpha cq}$, $I_{\beta cq}$ and the active power compensation degree γ are obtained. Through the calculation of the command current, the reference command currents of the converters VSC_α and VSC_β and bidirectional DC/DC in the ESRPC can be obtained.

Assuming that the ratio of the primary and secondary sides of the step-down transformer T_α and T_β are both k_T, the reference command currents of VSC_α and VSC_β according to (8) and (9) are:

$$\begin{cases} i^*_{\text{ric}\alpha}(t) = k_T \left[0.5 \left(I_{\text{sav z}} - \gamma (I_{\text{L}\alpha\text{d}} - I_{\text{L}\beta\text{d}}) \right) \sin \omega t + I_{\alpha cq} \cos \omega t \right] \\ i^*_{\text{ric}\beta}(t) = k_T \left[0.5 \left(I_{\text{sav z}} + \gamma (I_{\text{L}\alpha\text{d}} - I_{\text{L}\beta\text{d}}) \right) \sin \omega t + I_{\beta cq} \cos \omega t \right] \end{cases}, \qquad (14)$$

where ωt is the fundamental angular frequency, which can be obtained from the voltages of the two power supply arms through the phase-locked loop.

Suppose the terminal voltage of the energy storage medium is U_{sav}, and according to the conservation of active power, the reference command current of the bidirectional DC/DC can be expressed as:

$$I^*_{\text{sav}} = \frac{U_\alpha I_{\text{sav z}}}{U_{\text{sav}}} . \qquad (15)$$

The obtained command current of each converter is used to control the action of each converter switch tube, so that the actual output current can track the command current. At present, there are many literatures on RPC and bidirectional DC/DC converter control methods [14, 17]. Due to space limitations, this article will not discuss them in detail.

5. Test verification and analysis

In order to verify the effectiveness of the proposed strategy, a simulation model was built in MATLAB/Simulink according to the ESRPC topology structure shown in Fig. 1, and the simulation results of the ESRPC under typical operating conditions were analyzed. The simulation model parameter settings are shown in Table 1.

Through the preset working conditions, the load power changes of α and β power supply arms are shown in Fig. 4(a). ①~⑤ in the figure correspond to the five typical working conditions in Table 2. The compensation power of the energy storage RPC system under different working conditions is shown in Fig. 4(b), the power of the traction substation before and after compensation is shown in Fig. 4(c), and the state of charge change of the energy storage medium supercapacitor is shown in Fig. 4(d).

Table 1. The simulation model parameters

System type	Parameters	Symbol	Values	Unit
Traction substation	V/v transformer ratio	k	110/27.5	–
	Substation capacity	–	40	MVA
RPC system	Step-down transformer ratio	k_T	27.5/1.5	–
	RPC device capacity	S_{RPC}	4	MVA
	Filter inductance	L_s	0.6	mH
	Support capacitor	C	10e–3	F
	Intermediate DC side voltage	U_{dc}	3500	V
Energy storage system	DC/DC equipment capacity	–	2	MW
	Energy storage medium	–	Super capacitor	–
	Energy storage capacity	–	0.07	MWh
	Super capacitor capacitance	–	140	F
	Charge threshold	$I_{lim L}$	0.5	MW
	Discharge threshold	$I_{lim H}$	4	MW
	Depth of charge and discharge	–	10%–95%	–
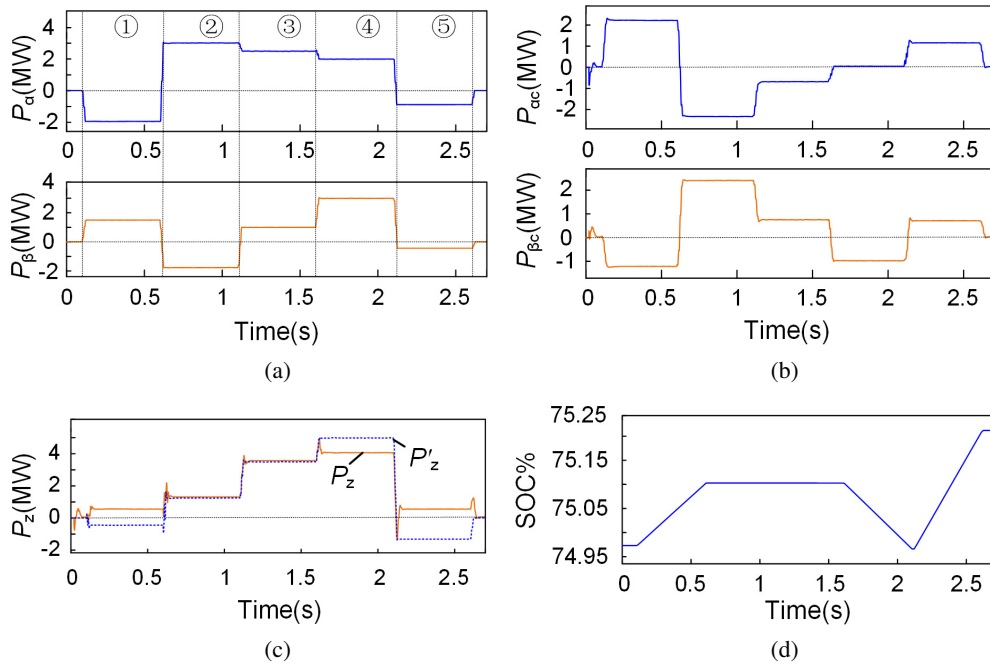
Fig. 4. Compensation of ESRPC system under different typical working conditions: load active power of two power supply arms (a); ESRPC compensation active power (b); traction substation power before and after ESRPC compensation (c); SOC of energy storage medium (d)

Table 2. Setting of typical operating conditions

Working conditions	$I_{L\alpha d}$/MW	$I_{L\alpha q}$/Mvar	$I_{L\beta d}$/MW	$I_{L\beta q}$/Mvar
1	−1.95	−1.02	1.50	0.76
2	2.98	1.49	−1.77	−0.93
3	2.49	2.03	1.00	0.51
4	2.00	1.03	3.00	1.51
5	−0.88	−0.46	−0.44	−0.23

In Fig. 4(c), P_z is the total power provided by the traction substation for the load before compensation, and P'_z is the total power provided by the traction substation after compensation. It can be seen from Figs. 4(b), 4(c) that the energy storage RPC system always has good dynamic performance during the entire compensation process. The specific analysis of the negative sequence compensation and power compensation effects under each working condition is as follows.

A. Working condition 1

In working condition 1, the α power supply arm is in the regenerative braking condition, the β power supply arm is in the traction condition, and the regenerative braking power is greater than the traction power 0.45 MW. At this time, the energy storage system absorbs excess regenerative braking energy and at the same time increases the power above the set charging threshold. It can be seen from Fig. 4(b) that the charging power of the energy storage system is 0.99 MW. The three-phase side current waveforms and amplitude changes of the traction substation before and after compensation are shown in Fig. 5. The simulation results of working condition 1 are shown in Table 3. The negative sequence current is reduced from 3.747 A before compensation to 0.106 A after compensation, and the power factor is increased from 0.853 before compensation to 0.998.
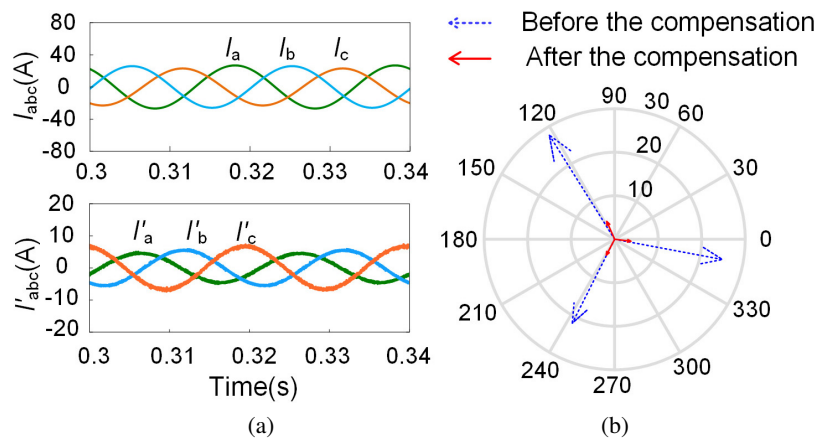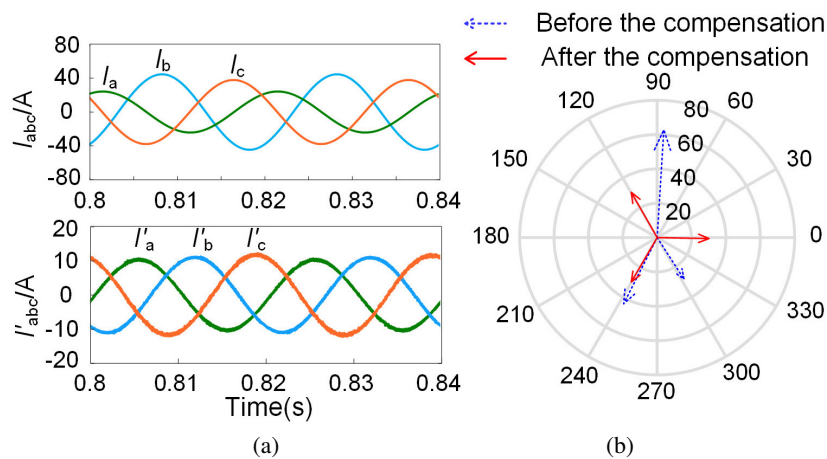

Fig. 5. Condition 1: three-phase current before and after compensation (a); three-phase current vector diagram before and after compensation (b)

It means that the proposed strategy not only can effectively recover regenerative braking energy, but also has good negative sequence compensation and power factor compensation capabilities.

Table 3. Simulation results of working condition 1

	I_{a2}/A	Q_{PF}
Before the compensation	3.747	0.853
After the compensation	0.106	0.998

B. Working condition 2

In working condition 2, the α power supply arm is in traction mode and the β power supply arm is in regenerative braking mode. At this time, the traction power is greater than a regenerative braking power of 1.21 MW. The energy storage RPC system only needs to compensate for the negative sequence and the energy storage system is in a standby state. The simulation results of working condition 2 are shown in Table 4. It can be seen from Fig. 6 and Table 4 that after compensation, the negative sequence current on the three-phase side of the traction substation is reduced from the original 5.366 A to 0.021 A, and the power factor is increased from the original

Table 4. Simulation results of working condition 2

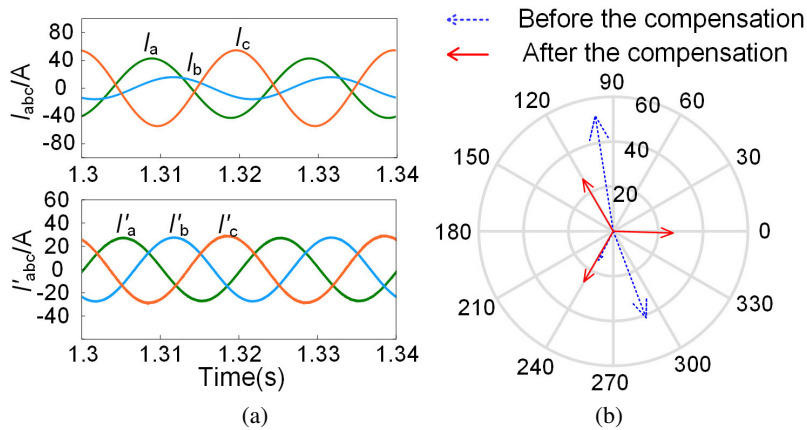|	I_{a2}/A	Q_{PF}
Before the compensation	5.366	0.908
After the compensation	0.021	0.999

Fig. 6. Condition 2: three-phase current before and after compensation (a); three-phase current vector diagram before and after compensation (b)

0.908 to 0.999. The energy storage system is neither charged nor discharged. At the same time, it can be seen from Fig. 4(d) that the energy storage system has no additional power loss during standby.

C. Working condition 3

In working condition 3, the two power supply arms α and β are in traction mode at the same time, the total traction power is 3.49 MW, and the traction power of the α power supply arm is greater than that of the β power supply arm. At this time, the ESRPC system only balances the active power of the two arms, without charging and discharging, and the energy storage system is in a standby state. The simulation results of working condition 3 are shown in Table 5. It can be seen from Fig. 7 and Table 5 that after compensation, the negative sequence current on the three-phase side of the traction substation is reduced from the original 5.676 A to 0.132 A, and the power factor is increased from the original 0.808 to 1.

Table 5. Simulation results of working condition 3

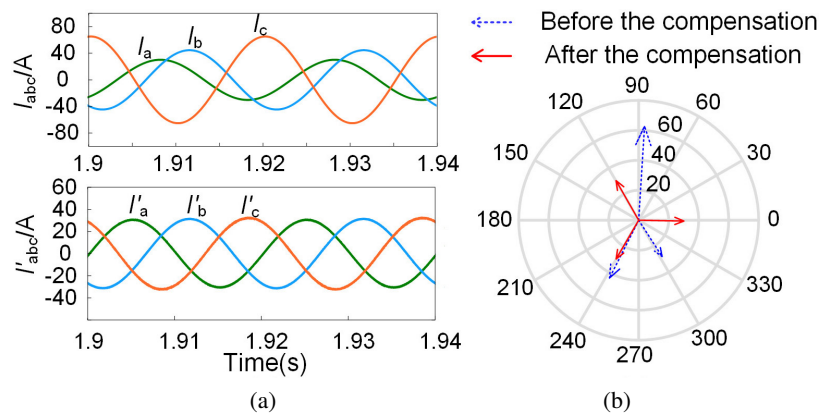|	I_{a2}/A	Q_{PF}
Before the compensation	5.676	0.808
After the compensation	0.132	1.000

Fig. 7. Condition 3: three-phase current before and after compensation (a); three-phase current vector diagram before and after compensation (b)

D. Working condition 4

In working condition 4, the two power supply arms α and β are in traction working condition at the same time, and the total traction power is 5 MW, which is greater than the set peak-shaving discharge threshold. While compensating for the negative sequence, the ESRPC system also provides a portion of power for the loads of the two power supply arms. The simulation results of working condition 4 are shown in Table 6. It can be seen from Fig. 8 and Table 6. that after

the ESRPC system is compensated, the negative sequence current on the three-phase side of the traction substation is reduced from the original 5.520 to 0.071, and the power factor is increased from the original 0.891 to 1. The discharge power of the energy storage system is 0.966 MW. While performing negative sequence compensation, it can also compensate part of the traction power, reducing the power demand of the traction load on the traction substation.

Table 6. Simulation results of working condition 4

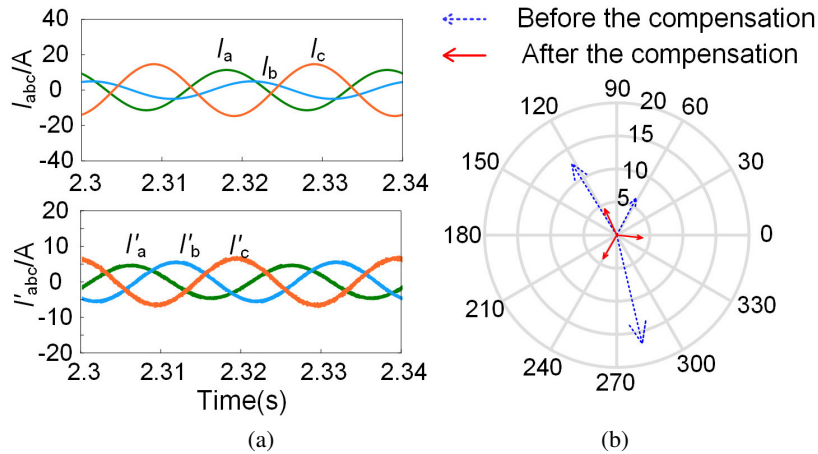|	I_{a2}/A	Q_{PF}
Before the compensation	5.520	0.891
After the compensation	0.071	1.000

Fig. 8. Condition 4: three-phase current before and after compensation (a); three-phase current vector diagram before and after compensation (b)

E. Working condition 5

In working condition 5, the α and β power supply arms are regeneratively braked at the same time, and the total regenerative braking power reaches –1.32 MW. The energy storage type RPC system needs to fully recover the regenerative braking energy and raise the power level of the power supply arm above the valley filling charging threshold. It also needs to compensate for the negative sequence on the three-phase side of the traction substation. It can be seen from Fig. 4(c), 4(d) that the energy storage system is charged and the charging power is 1.824 MW. Fig. 9 is the current waveform and amplitude diagram of the three-phase side of the traction substation. The simulation results of working condition 5 are shown in Table 7. It can be seen that after compensation, the negative sequence current is reduced from the original 1.596 A to 0.067 A, and the power factor is increased from the original 0.884 to 0.997.

The running environment of the simulation model is based on AMD R7 4800U, 12 GB, and the maximum delay of program running is 17 ms. It can satisfy the calculation requirement of real-time compensation.

Table 7. Simulation results of working condition 5

	I_{a2}/A	Q_{PF}
Before the compensation	1.596	0.884
After the compensation	0.067	0.997

Fig. 9. Condition 5: three-phase current before and after compensation (a); three-phase current vector diagram before and after compensation (b)

6. Conclusions

Aiming at the problems of negative sequence control and regenerative braking energy recovery as well as the utilization of electrified railways, the mechanism of negative sequence compensation and regenerative braking energy utilization of the ESRPC is analyzed, and an ESRPC layered compensation optimization strategy is proposed that takes into account the production of the energy storage system under limited equipment capacity. When the system capacity is limited, this strategy can consider the balance among renewable energy recovery, negative sequence management and power factor compensation. It makes full use of the system capacity to achieve the purpose of optimizing compensation, and has good real-time performance. The device capacity optimization of the ESRPC system will be the focus of future research.

References

[1] Aguado J.A., Sánchez Racero A.J., de la Torre S., *Optimal operation of electric railways with renewable energy and electric storage systems*, IEEE Transactions on Smart Grid, vol. 9, no. 2, pp. 993–1001 (2018), DOI: 10.1109/TSG.2016.2574200.

[2] Deng Y., Lin Z., *Thoughts on challenges faced by Sichuan-Tibet railway electrification project and its solutions*, Electrified Railway, vol. 30, no. S1, pp. 5–11+15 (2019), DOI: 10.19587/j.cnki.1007-936x.2019z.002.

[3] Roudsari H.M., Jalilian A., Jamali S., *Flexible fractional compensating mode for railway static power conditioner in a V/v traction power supply system*, IEEE Transactions on Industrial Electronics, vol. 65, no. 10, pp. 7963–7974 (2018), DOI: 10.1109/TIE.2018.2801779.

[4] Dai N.Y., Lao K., Lam C., *Hybrid railway power conditioner with partial compensation for converter rating reduction*, IEEE Transactions on Industry Applications, vol. 51, no. 05, pp. 4130–4138 (2015), DOI: 10.1109/TIA.2015.2426134.

[5] Jiang Y., Liu X., Zhao L., Wang Z., Cao Y., *Research on Stability and Control Strategy of Railway Power Conditioner*, Power System Technology, vol. 42, no. 05, pp. 1620–1627 (2018), DOI: 10.13335/j.1000-3673.pst.2017.2852.

[6] Zhang D., Zhang Z., Wang W., Yang Y., *Negative sequence current optimizing control based on railway static power conditioner in v/v traction power supply system*, IEEE Transactions on Power Electronics, vol. 31, no. 1, pp. 200–212 (2016), DOI: 10.1109/TPEL.2015.2404934.

[7] Alfieri L., Battistelli L., Pagano M., *Impact on railway infrastructure of wayside energy storage systems for regenerative braking management: a case study on a real Italian railway infrastructure*, IET Electrical Systems in Transportation, vol. 9, no. 03, pp. 140–149 (2019), DOI: 10.1049/iet-est.2019.0005.

[8] Zhang Z., Zhang B., Wang D., Li P., Rong Y., *Battery/super-capacitor HESS applied in DC microgrid*, Archives of Electrical Engineering, vol. 69, no. 2, pp. 379–388 (2020), DOI: 10.24425/aee.2020.133032.

[9] Jayalakshmio N.S., Gaonkar D.N., Karthik R.P., Prasann P., *Intermittent power smoothing control for grid connected hybrid wind/PV system using battery-EDLC storage devices*, Archives of Electrical Engineering, vol. 69, no. 2, pp. 433–453 (2020), DOI: 10.24425/aee.2020.133036.

[10] Ma Q., Guo X., Luo P., Zhang Z., *A novel railway power conditioner based on super capacitor energy storage system*, Transactions of China Electrotechnical Society, vol. 33, no. 06, pp. 1208–1218 (2018), DOI: 10.19595/j.cnki.1000-6753.tces.161986.

[11] Ma F., Wang X., Deng L., Zhu Z., Xu Q., Xie N., *Multiport railway power conditioner and its management control strategy with renewable energy access*, IEEE Journal of Emerging and Selected Topics in Power Electronics, vol. 8, no. 2, pp. 1405–1418 (2020), DOI: 10.1109/JESTPE.2019.2899138.

[12] Hu H., Chen J., Ge Y., Huang W., Liu L., He Z., *Research on regenerative braking energy storage and utilization technology for high-speed railways*, Proceedings of the CSEE, vol. 40, no. 1, pp. 246–256+391 (2020), DOI: 10.13334/j.0258-8013.pcsee.190650.

[13] Wei W., Hu H., Wang K., Chen J., He Z., *Energy storage scheme and control strategies of high-speed railway based on railway power conditioner*, Transactions of China Electrotechnical Society, vol. 34, no. 6, pp. 1290–1299 (2019), DOI: 10.19595/j.cnki.1000-6753.tces.180287.

[14] Cui G., Luo L., Liang C., Hu S., Li Y., Cao Y., Xie B., Xu J., Zhang Z., Liu Y., Wang T., *Supercapacitor integrated railway static power conditioner for regenerative braking energy recycling and power quality improvement of high-speed railway system*, IEEE Transactions on Transportation Electrification, vol. 5, no. 3, pp. 702–714 (2019), DOI: 10.1109/TTE.2019.2936686.

[15] Şengör İ., Kılıçkıran H.C., Akdemir H., Bedri Kekezoğlu B., Erdinç O., Catalão J.P.S., *Energy management of a smart railway station considering regenerative braking and stochastic behaviour of ESS and PV generation*, IEEE Transactions on Sustainable Energy, vol. 9, no. 3, pp. 1041–1050 (2018), DOI: 10.1109/IS3C.2018.00121.

[16] Sheng W., Cheng S., Liu K., *Optimal control of distribution network containing distributed generations based on trust region sequential quadratic programming algorithm*, Power System Technology, vol. 38, no. 3, pp. 662–668 (2014), DOI: 10.13335/j.1000-3673.pst.2014.03.018.

[17] Wang Q., Liu Y., Song W., Xuan K., *Improved dynamic control method for energy storage units in PV dominated microgrids*, Archives of Electrical Engineering, vol. 67, no. 4, pp. 885–898 (2018), DOI: 10.24425/aee.2018.124747.